MAE 4223

Aerospace Engineering Laboratory

Wind Tunnel Airfoil Measurements

DATE DUE: 3-15-2001

BY: Charles O'Neill

TABLE OF CONTENTS

ABSTRACT

A wing is experimentally tested in a low speed wind tunnel at Mach 0.075. Basic wing theory is reviewed. Lift and drag were measured from zero lift to stall. A lift curve and drag polar are calculated. The experimental lift curve slope was accurately predicted by Glauert's finite wing theory. Errors in measurements and the effect on uncertainty are discussed.

LIST OF FIGURES

INTRODUCTION

An experimental wing is tested in a wind tunnel. The equipment and procedures for testing a wing in the OSU low speed wind tunnel will be discussed. Basic wing theory will be reviewed to assist with the quantification of the wing's performance. Uncertainty will be discussed. The stall characteristics will be observed and discussed.

EQUIPMENT

The equipment used for this experiment consisted of a low-speed wind tunnel, measurement equipment and and experimental wing.

The wind tunnel used was the MAE low speed tunnel in the North Lab (ME). The wind tunnel has 36 inch square test section. A glass window is installed on both the top and one side for observation. Figure 1 shows the general layout of the wind tunnel.

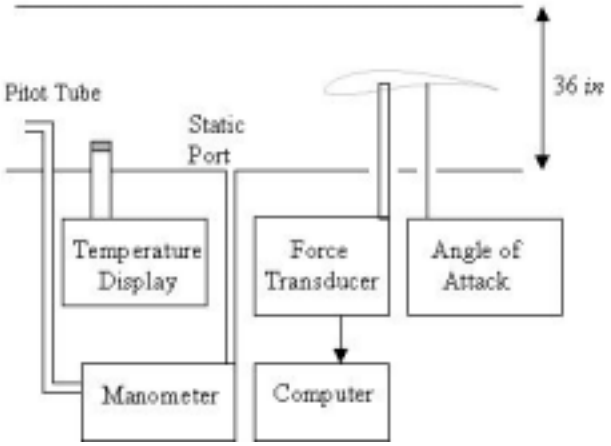

Figure 1. Test Equipment

The measurement equipment consists of transducers to measure air properties and wing forces. A digital temperature gage is installed upstream of the test section. A manometer is connected to a pitot static system to set the wind tunnel velocity. Resulting forces are measured with a six axis force balance; however, only the lift and drag forces were used. The force balance is connected to a computer display and recording system. Angle of attack is varied with a control arm mounted on the force balance. An analog counter displays the angle of attack within a 0.1 degree resolution.

PROCEDURE

This wing test experiment requires three steps. First, local air properties are determined. Barometric pressure is recorded and corrected for temperature and local gravity. Next, the force balance is calibrated. The transducer output is recorded for a series of test weights. The wing is mounted on the force balance system at zero degrees. The wind tunnel is run up to 1.5 inches of water. Finally, the wing is tested at various angles of attack. Initially, angle of attack is reduced to the point of zero lift. Then, the

angle of attack is increased to past the stall. Data points are taken for 1 and 2 degree increments of angle of attack.

THEORY

A simple relationship between water height and pressure for manometers is derived from Bernoulli's equation.

$$\Delta P = \tfrac{1}{2}\rho V^2$$

Rearranging yields,

$$V = \sqrt{\frac{2\Delta P}{\rho}}$$

Adding the pressure due to height, $\Delta P = \rho_{H_2O} g h$, yields,

$$V = \sqrt{\frac{2\rho_{H_2O} g h}{\rho}}$$

As seen above, only the ratio between the densities of the manometer fluid and air are important in the velocity measurement. From Kuethe [1] the density of water is 1000 kg/m^3.

Basic wing theory quantifies a wing's characteristics. Aspect ratio is defined as,

$$AR = b^2 / S$$

To increase their usefulness, airfoil forces are non-dimensionalized. Lift is non-dimensionalized to lift coefficient by,

$$L = qSC_L$$

Drag is non-dimensionalizezd to a drag coefficient by,

$$D = qSC_D$$

Where q is the dynamic pressure and S is the planform area.

Glauert's wing approximation gives an estimate of the lift curve slope.

$$\frac{dC_L}{d\alpha} = \frac{C_{l\alpha}}{1 + (57{,}3C_l / \pi\, AR)(1+\tau)}$$

α_{0l} is the zero lift angle of attack and τ is a planform shape parameter. For this experiment, τ is assumed to be zero. This equation has been modified from the handout.

RESULTS

Measurements were performed as given above. Raw Data is given in Tables 1 and 2 in the appendix. The wing was tested at a wind tunnel pitot pressure of 1.5 inches of water. This is approximately 82 feet per second or Mach 0.075. The average Reynolds number of the wing is 139000. The wing planform area is 57.38 square inches. The span is 18 inches with a root chord of 4.25 inches and a tip chord of 2.125 inches. The root airfoil section is a Selig 1223 and the tip is a N.A.C.A 0009. From wing geometry theory, the aspect ratio is 5.6 with a 0.5 taper ratio.

The force balance was calibrated as described above for lift and drag. Best-fit lines were derived from the data points given in Table 1. A plot of the data points and the best-fit line for the lift axis is given in Figure 2. A plot of the drag data points and the best-fit line is given in Figure 3. The lift best fit lines are described by,

$$Lift[g] = 18774\,\text{Output} - 192.36$$

$$\text{Drag[g]} = 13238\,\text{Output} + 6314.6$$

One outlier, shaded black in Figure 3, was deleted from the drag best-fit line.

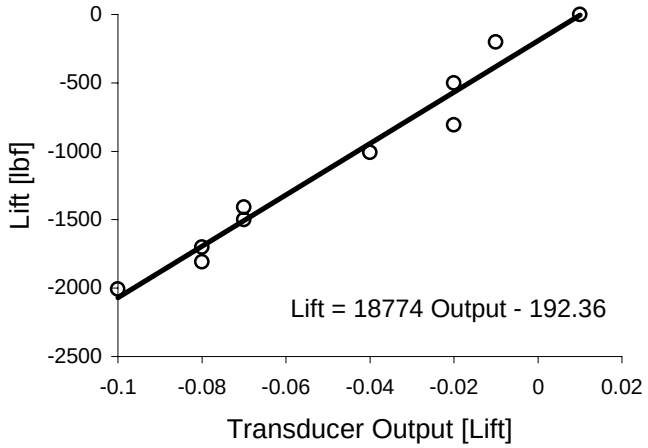

Figure 2. Lift Calibration

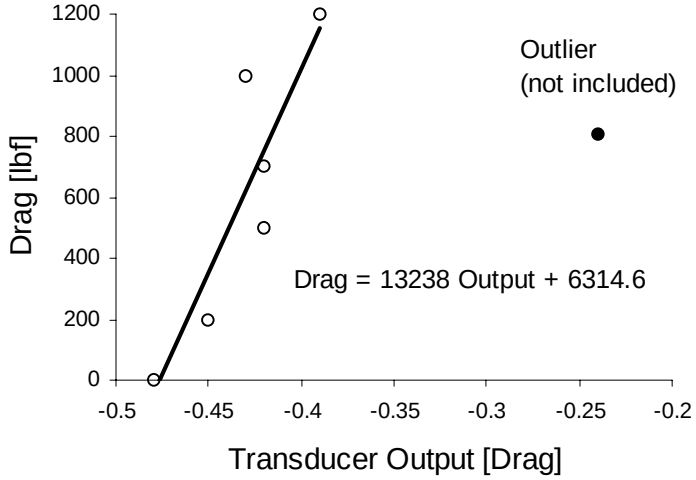

Figure 3. Drag Calibration

Lift and Drag measurements were performed as described above. Raw lift and drag transducer output values are given in Table 3. Data values calculated from the calibration curves are given in Table 4.

Experimental uncertainty is estimated by considering the uncertainty in the measurements. For the force balance, the calibration related weight and a computer display output. From above, the lift is given by,

$$Lift\,[g] = 18774\,\text{Output} - 192.36$$

The output is assumed had a readout resolution of within ±0.01 for calibration and the calibration weights are known to ±1 gram. Thus, the worst-case estimates of the lift are,

$$Lift\,[g] = 18774\,(\text{Output} \pm 0.01) - 192.36 \pm 1.0$$

At an angle of attack of 0, the lift output is 0.085. The minimum lift estimate as determined by uncertainty analysis is,

$$Lift\,[g] = 18774\,(\text{Output} \pm 0.01) - 192.36 \pm 1.0$$

$$\text{Lift}\,[\text{g}] = 18774(0.085 - 0.01) - 192.36 - 1.0$$

$$\text{Lift}\,[\text{g}] = 1215\,\text{g}$$

$$\text{Lift}\,[\text{lbf}] = 2.67\,\text{lbf}$$

Likewise, the maximum lift estimate is,

$$Lift\,[g] = 18774\,(\text{Output} \pm 0.01) - 192.36 \pm 1.0$$

$$\text{Lift}\,[\text{g}] = 18774(0.085 + 0.01) - 192.36 + 1.0$$

$$\text{Lift}\,[\text{g}] = 1592\,\text{g}$$

$$\text{Lift}\,[\text{lbf}] = 3.5\,\text{lbf}$$

Thus, the estimated lift at zero angle of attack considering the uncertainty of measurement and calibration is,

$$Lift = 3.09 \pm 0.415\,lbf$$

Similarly for drag, the worst case estimates at zero angle of attack are,

$$\text{Drag}[\text{g}] = 13238\,(\text{Output} \pm 0.01) + 6314.6 \pm 1.0$$

At an angle of attack of 0, the drag output is –0.45. The minimum drag estimate as determined by uncertainty analysis is,

$$\text{Drag}[\text{g}] = 13238\,(-.45 - 0.01) + 6314.6 - 1.0$$

$$\text{Drag}\,[\text{g}] = 224\,\text{g}$$

$$\text{Drag}\,[\text{lbf}] = 0.49\,\text{lbf}$$

Likewise, the maximum drag estimate is,

$$\text{Drag}[\text{g}] = 13238\,(-.45 + 0.01) + 6314.6 + 1.0$$

$$\text{Drag}\,[\text{g}] = 491\,\text{g}$$

$$\text{Drag}\,[\text{lbf}] = 1.08\,\text{lbf}$$

Thus, the estimated drag at zero angle of attack considering the uncertainty of measurement and calibration is,

$$Lift = .785 \pm 0.295\,lbf$$

This is an uncertainty of 38 percent for drag. This is an unacceptable amount of uncertainty.

Clearly, the uncertainty is too high. This is partially due to the low output resolution, 0.01, during the calibration. After calibration, the display program, LabView, was investigated. This resulted in chaging the resolution by a factor of 3 to 0.00001.

Lift data was non-dimensionalized and plotted in Figure 4 versus angle of attack. The zero lift angle of attack is –8.5 degrees. The lift curve slope is 0.088 1/deg. From Glauert's approximation, theory predicts a lift curve slope of 0.081 1/deg. Clmax is 1.92 at 14 degrees. The linear portion of the lift curve goes to 8 degrees.

As expected, the lift curve has a linear region at low angles of attack, a roll off at higher angles of attack and a maximum near the universal 15 degree stall region. Experimental values for the lift curve slope agree with theory.

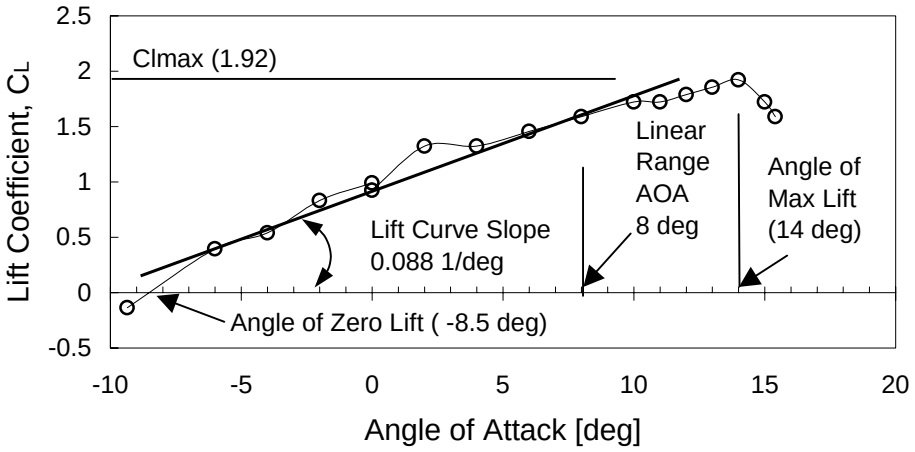

Figure 4. Wing Lift Curve

A drag polar was computed from the lift and drag coefficients and is given in Figure 5. Unfortunately, the drag values are not consistent. Ignoring the shaded points helps to discern the expected trend.

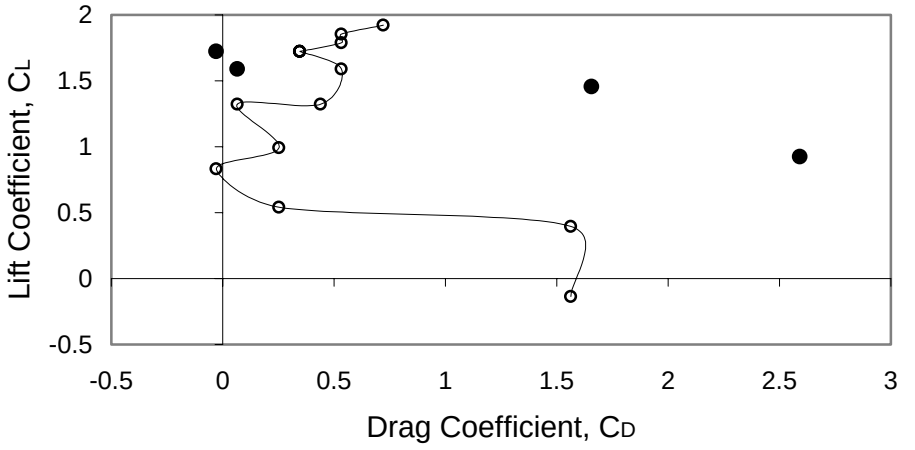

Figure 5. Wing Drag Polar

From the UIUC low speed airfoil website, the Selig 1223 at a Reynolds number of 150000 has a drag polar as given in Figure 6. The OSU tested wing is a combination of a

Selig 1223 and a N.A.C.A 0009, so the polars are expected to have different values. However, both polars show the sharp increase in drag below a lift coefficient of 1.0. Thus, the 1223 is probably the major influence on lift at low angles of attack.

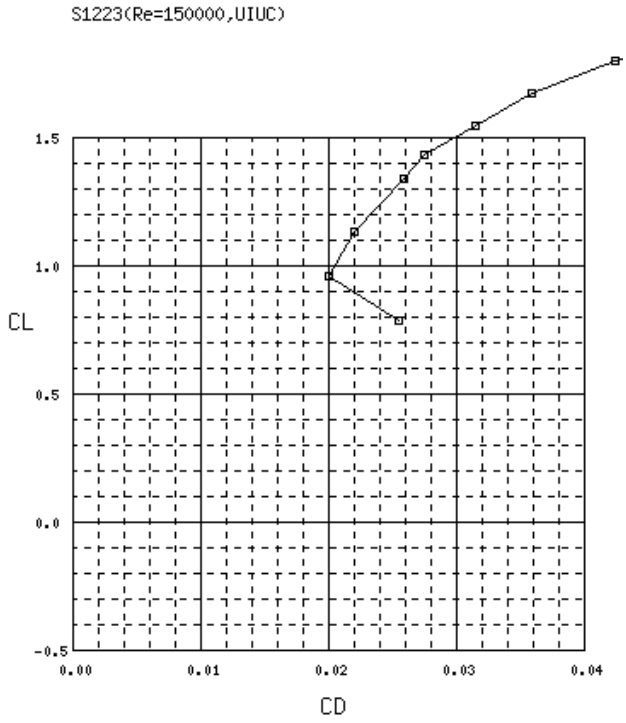

Figure 6. Selig 1223 Drag Polar

The wing's upper surface was tufted to allow flow visualization. Separated regions are spotted by the tufts moving off the wing surface. In some cases, the tufts vibrate or rotate. Stall separation first occurred at the root at about 10 degrees. Also, at the 70 percent halfspan, the local wing area was stalled. As the angle of attack increased, the separated region at the root moved towards the wingtip. Past Clmax, the entire wing was separated.

CONCLUSIONS AND RECOMMENDATIONS

The following conclusions and recommendations are proposed,

1. The slope of the lift curve was accurately predicted by the Glauert approximation.
2. The experimental drag polar is similar to the root airfoil's drag polar
3. Calibration resolution was too low. This was fixed before beginning the experimental measurements. Inaccuracies in drag measurements were problematic throughout the subsequent data analysis.
4. The data recording system needs to be set to higher resolution throughout the experiment.
5. The stall pattern is as expected for a tapered and twisted wing. The separation started at the root and progressed to the tip as the angle of attack increased.

REFERENCES

1. Kuethe, A. M., and Chow, Chuen-Yen., "Table 2. Properties of Air and Water," *Foundations of Aerodynamics*, 5th ed., Wiley, New York, 1998, p. 532.

APPENDICES

SAMPLE CALCULATIONS

1. Conversion from Transducer Output to Weight

$$T = Constant \cdot Voltage$$
$$T = 3.8082(1000\,mV)$$
$$T = 2808.2\,gram$$
$$T = \frac{2808.2\,gram}{454\,gram/lb}$$
$$T = 6.185\,lb$$

2. Velocity Conversion from Pressure

$$V = \sqrt{\frac{2\rho_{H_2O} gh}{\rho}}$$
$$V = \sqrt{\frac{(2)(1000\,\mathrm{kg/m^3})(32.2\,\frac{ft}{s^2})(1.5\,in)}{(12\,\frac{in}{ft})(1.172\,\mathrm{kg/m^3})}}$$
$$V = 82.877\,\frac{ft}{s}$$

3. Dynamic Pressure Conversion

$$q = \rho\, g\, h$$
$$q = 1.5\,in\,H_2O$$
$$q = (1000\,kg/m^3)(32.2\ ft/s^2)(1.5\,in\,H_2O)(\frac{0.225\,lbf\,s^2}{kg\,m})(\frac{m}{39.37in})^4(\frac{12\,in}{ft})$$
$$q = 0.0542\ psi$$

4. Air Density

$$\rho = \frac{P}{RT}$$
$$\rho = \frac{(97.57\,KPa)}{(287\,m^2/s^2/K)(290\,K)}$$
$$\rho = 1.172\ \mathrm{kg/m^3}$$
$$\rho = 1.316 \cdot 10^{-6}\ \mathrm{slug/in^3}$$

5. Glauert's Finite Wing Approximation

$$\frac{dC_L}{d\alpha} = \frac{C_{l\alpha}}{1 + (57{,}3\,C_l/\pi\,AR)(1+\tau)}$$
$$\frac{dC_L}{d\alpha} = \frac{2\pi/57.3}{1 + (2\pi/\pi\,AR)(1)} = 0.081\,\frac{1}{\mathrm{deg}}$$

SPREADSHEET TABLES

TABLE 1. Raw Calibration Data

Lift		Drag	
Output	Weight [g]	Output	Weight [g]
0.01	0	-0.48	0
-0.01	-200	-0.45	200
-0.02	-500	-0.42	500
-0.02	-807	-0.42	700
-0.04	-1007	-0.43	1000
-0.07	-1407	-0.39	1200
-0.07	-1500		
-0.08	-1700	-0.24	807
-0.08	-1807		
-0.1	-2007		

TABLE 2. Raw Force Data

in H20	1.5
Temp [C]	16.3

AOA index	Drag Output	Lift Output
72	-0.45	0.085
52	-0.48	0.073
32	-0.45	0.051
12	-0.31	0.04
-21.5	-0.31	0
72	-0.2	0.08
92	-0.47	0.11
112	-0.43	0.11
132	-0.3	0.12
152	-0.42	0.13
172	-0.44	0.14
182	-0.44	0.14
192	-0.42	0.145
202	-0.42	0.15
212	-0.4	0.155
222	-0.48	0.14
226	-0.47	0.13

TABLE 3. Raw Lift and Drag Data

in H20	1.5
Temp [C]	16.3

AOA index	Drag Output	Lift Output
72	-0.45	0.085
52	-0.48	0.073
32	-0.45	0.051
12	-0.31	0.04
-21.5	-0.31	0
72	-0.2	0.08
92	-0.47	0.11
112	-0.43	0.11
132	-0.3	0.12
152	-0.42	0.13
172	-0.44	0.14
182	-0.44	0.14
192	-0.42	0.145
202	-0.42	0.15
212	-0.4	0.155
222	-0.48	0.14
226	-0.47	0.13

TABLE 4. Calculated Lift and Drag Data

Lift	18774x +	-192.36		Air Density [slug/in3]	1.32E-06
Drag	13238x +	6314.6		Dynamic Press [psi]	0.0543
				Wing Area [in2]	57.38

AOA	Lift grams	Lift lbf	Drag grams	Drag lbf	AOA	CL	CD
0	1403.43	3.091256	357.5	0.787445	0	0.992144	0.252732
-2	1178.142	2.595026	-39.64	-0.08731	-2	0.832878	-0.02802
-4	765.114	1.685273	357.5	0.787445	-4	0.540891	0.252732
-6	558.6	1.230396	2210.82	4.869648	-6	0.394898	1.562921
-9.35	-192.36	-0.4237	2210.82	4.869648	-9.35	-0.13599	1.562921
0	1309.56	2.884493	3667	8.077093	0	0.925783	2.592356
2	1872.78	4.125066	92.74	0.204273	2	1.323947	0.065562
4	1872.78	4.125066	622.26	1.370617	4	1.323947	0.439902
6	2060.52	4.53859	2343.2	5.161233	6	1.456668	1.656506
8	2248.26	4.952115	754.64	1.662203	8	1.589389	0.533487
10	2436	5.365639	489.88	1.079031	10	1.722111	0.346317
11	2436	5.365639	489.88	1.079031	11	1.722111	0.346317
12	2529.87	5.572401	754.64	1.662203	12	1.788471	0.533487
13	2623.74	5.779163	754.64	1.662203	13	1.854832	0.533487
14	2717.61	5.985925	1019.4	2.245374	14	1.921193	0.720657
15	2436	5.365639	-39.64	-0.08731	15	1.722111	-0.02802
15.4	2248.26	4.952115	92.74	0.204273	15.4	1.589389	0.065562